 doi:10.20944/preprints202106.0426.v1

COMPACT WAVELENGTH SELECTIVE CROSSBAR SWITCH WITH CASCADED FIRST ORDER MICRO-RING RESONATORS

A PREPRINT

Akhilesh S. P. Khope, Robert Zhang, Roger Helkey, Rod C. Alferness, Adel A. M. Saleh, John E. Bowers
Electrical and Computer Engineering Department
University of California
Santa Barbara, CA 93106
akhkhope@gmail.com

June 16, 2021

ABSTRACT

We demonstrate a compact 4×4 wavelength selective switch with 50 % fewer electrical pads as compared with our previous generation. We report loss and crosstalk for different paths of the switch. We measure median loss of 5.32 dB and worst-case crosstalk of -35 dB. The microring resonators tune by more than one free spectral range, which is an improvement over our previous generation of switches. This switch can support 8 channels at 400 GHz spacing. We conclude that it is not possible to drive both microring resonators with the same voltage and separate control is required because of fabrication variation of the current technology.

Keywords Switching · Photonic Integrated Circuits · Optical Switching Devices

1 Introduction

Optical switches in datacenters reduce fiber handling and enable more scalable data centers [1]. A wavelength selective switch (WSS) can switch multiple wavelengths from an input port to output port [2]. WSS on silicon are reported in [3, 4, 5, 6, 7, 8, 9, 10, 11, 12]. Applications of these switches in HyperX datacenter topology is reported in [1]. We proposed a multi-wavelength selective crossbar switch (MSCS) in [13].

In this paper, we present a 4x4 switch with L = 2 (2 cascaded first order MRR at every crosspoint) switch that can tune over one full FSR with a more compact footprint. We also show full free spectral tuning of the MRR. MRR spectra are very sensitive to gap between waveguides. For the case of higher order ring resonators specific relationship between multiple coupling coefficients must be met for a flattop spectra. An easier approach to achieve a given 3 dB bandwidth and at the same time a higher out of band rejection is to cascade the drop transmission spectra of multiple first-order ring resonators. This results in a higher power penalty as compared to second order ring resonator, but the ease of design makes this one of the choices for the filter our switch.

4x4 switch with L = 2 with second-order cascaded first-order rings has up to 64 signal pads and the area of the switch scales as $2LN^2$. The area of this switch can be reduced by half if both of the ring resonator heaters are connected together. This places stringent constraints on acceptable resonant wavelength variation caused by the fabrication process. In this work, we measure a switch fabricated in a 220 nm Si Photonics foundry and report the standard deviation of loss, continuous wave (CW) crosstalk, resonant wavelength at zero bias, and full width at half maximum (FWHM).

Improvement in fabrication process will enable better scaling of future switches. We conclude that, switches cannot be designed by connecting the signals of the two ring resonators to the same pad with the current MRR uniformity across the chip. We compare two different chips and measure the dissimilarity between two rings by recording the voltage applied at the two rings.

Preprints (www.preprints.org) | NOT PEER-REVIEWED | Posted: 16 June 2021 doi:10.20944/preprints202106.0426.v1

2 Architecture

In this section, we describe the architecture of the switch. Fig 1 (a) shows a N $\times$ N switch with M wavelengths at each input port. We need only L = 2, i.e two MRR per crosspoint for near optimal latency [13]. Fig 1 (b) **Tx** corresponds to transmitter and **Rx** corresponds to receiver. Fig 1 (c) shows switch unit cell. Fig 1 (d) shows layout of a 4×4 (L = 2) switch. Fig 1 (e) shows micro graph of 4×4 (L = 2) switch. The MRR resonances are tuned using thermal tuning. We built the switch using MRR from AIM photonics process design kit (PDK).

During data transmission, time is divided into timeslots and at the start of every timeslot a centralized arbiter performs scheduling of traffic and wavelength assignment. More information about assignment and arbitration can be found in [4]. At the start of every timeslot the arbitration algorithm generates a traffic matrix. Each entry in the traffic matrix corresponds to number of wavelength channels required between input and output ports.

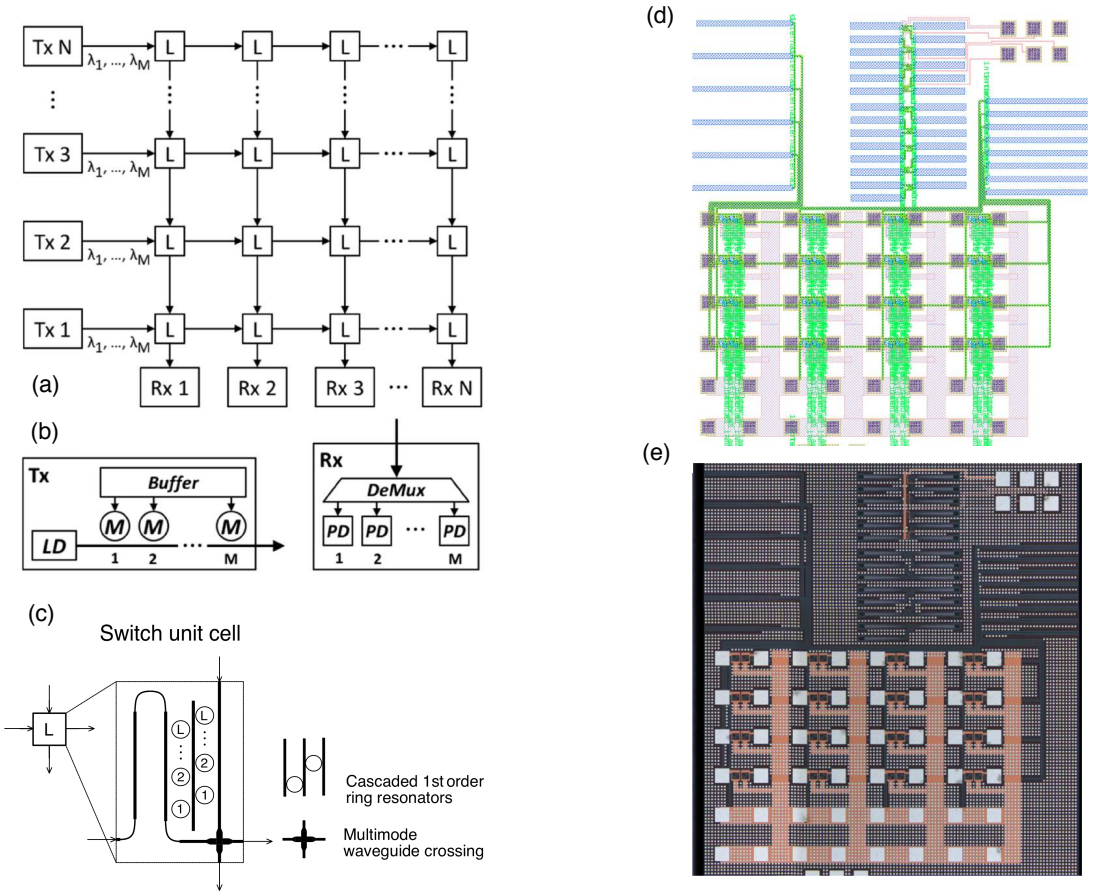

Figure 1: (a) NxN switch with L blocks. M wavelengths are input into the switch. (b) Tx: Transmitter, M microring modulators each driving one wavelength, Shared buffer so that data to any port can be modulated on any modulator.[13] (c) Contents on the L block. L cascaded first order microring resonators and waveguide crossing is used.(d) Layout of 4x4 switch and (e) Die shot of 4x4 switch

 doi:10.20944/preprints202106.0426.v1

3 Experimental Results

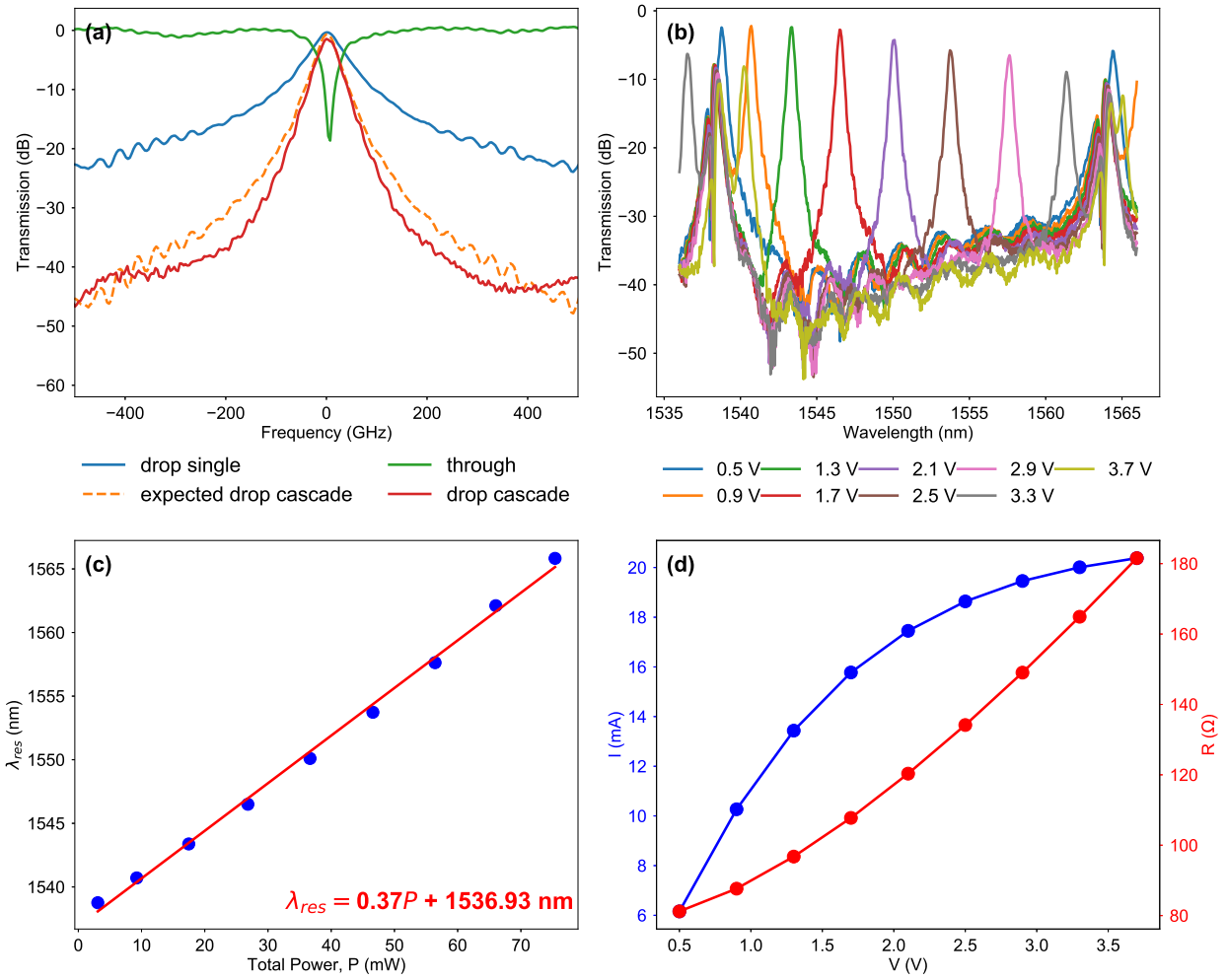

Figure 2: Measurements on cascaded first order ring resonator (a) Drop and through transfer spectra of a single first order ring resonator, Expected transfer spectra of cascaded order ring and the best measured cascaded ring, (b) Tuning curve of cascaded ring in a unit cell arrangement where bias is applied to only one ring,(c) Full FSR tuning is demonstrated. The ring tunes by 27.6 nm (> FSR = 25.6 nm) with power efficiency of 0.37 nm/mW for two rings.(d) IV and RV curves for the cascaded ring resonators. Nonlinear dependence of R vs. V is measured.

In this section, we report experimental results of the switch. Fig 2 (a) shows the measured transfer spectra comparison of one and two cascaded first-order ring resonators. The out-of-band rejection 400 GHz away from resonance wavelength of ring resonator increases from -21 dB to -40 dB as we change the ring filter from one to two cascaded filters. The 3-dB bandwidth of a single ring resonator is 64 GHz, from which we expect a 3-dB bandwidth of 38 GHz from the cascaded two-ring filters. This is the expected 3-dB bandwidth of the cascaded filters. The curve in red shows the measured cascaded filter response from one of the unit cells in the switch. However, as shown in the red curved in Fig 2 (a), the measured cascaded filter response from one of the unit cells in the switch has a 3-dB bandwidth of 40 GHz. This is due to the fact that the heaters of the two ring resonators are tied together. Thus, individual control of resonators is not possible and any misalignment between the resonators changes the filter shape. The extinction on the through port is -17 dB.

Fig 2(b) shows the tuning process of the cascaded first order ring filter. In this measurement, an increasing voltage is applied to one cascaded ring from a unit cell of the 4x4 switch. The ring tunes by 27.06 nm (Free Spectral Range (FSR) = 25.6 nm) with a tuning efficiency of 0.37 nm/mW (for both rings). This ring tunes by more than the FSR and thus can be used for selecting all WDM channels present in the system. The MRR can support 8 wavelength division

 doi:10.20944/preprints202106.0426.v1

multiplexed (WDM) channels at 400 GHz spacing. We automated the measurements with functions from Lumos, an instrument control library in python [14]. We use MRR from foundry process design kit (PDK) in this paper. We advise the reader to use MRR reported in [15] for a lower off resonance loss.

The low loss and full FSR tuning make this MRR an ideal candidate for opto-electronic switches. Tuning curve and Heater IV and RV are reported in Fig 2 (c) and (d). The tuning curve demonstrates full FSR tuning. The resonance wavelength is 1536.9 nm and the histogram of resonant wavelengths measured on different filters on the die is given in Fig 4. Heater IV in Fig 2 (d) shows that the current changes from 6 mA to 20 mA as the voltage changes from 0 to 3.7 mA. The resistance changes from 80 Ω to 180 Ω.

There are in total 32 signal pads and 16 ground pads with a total footprint of 1.6×1.55 mm^2. The signals were routed with a 1 µm/mA rule to avoid burnout due to electro migration. The layout was done with Cadence Virtuoso and waveguide crossings were designed using Phoenix Optodesigner. Traces of 70 µm and 20 µm are used to connect to the ground pads. Due to the low measured resistance of the ring resonators, traces with twice the width or connecting all grounds to a ground plane on a different electrical routing layer might be a better choice for future switches. Pad sizes are 60 µm $\times$ 60 µm with a pitch of 160 µm. A pitch of < 135 µm is unsuitable for flip-chip bonding to organic carriers and we choose this pitch even though we did not flip chip this chip in this work. All pads were filled with square vias, as larger number of vias connecting different pad layers prevent pad peel off problem.

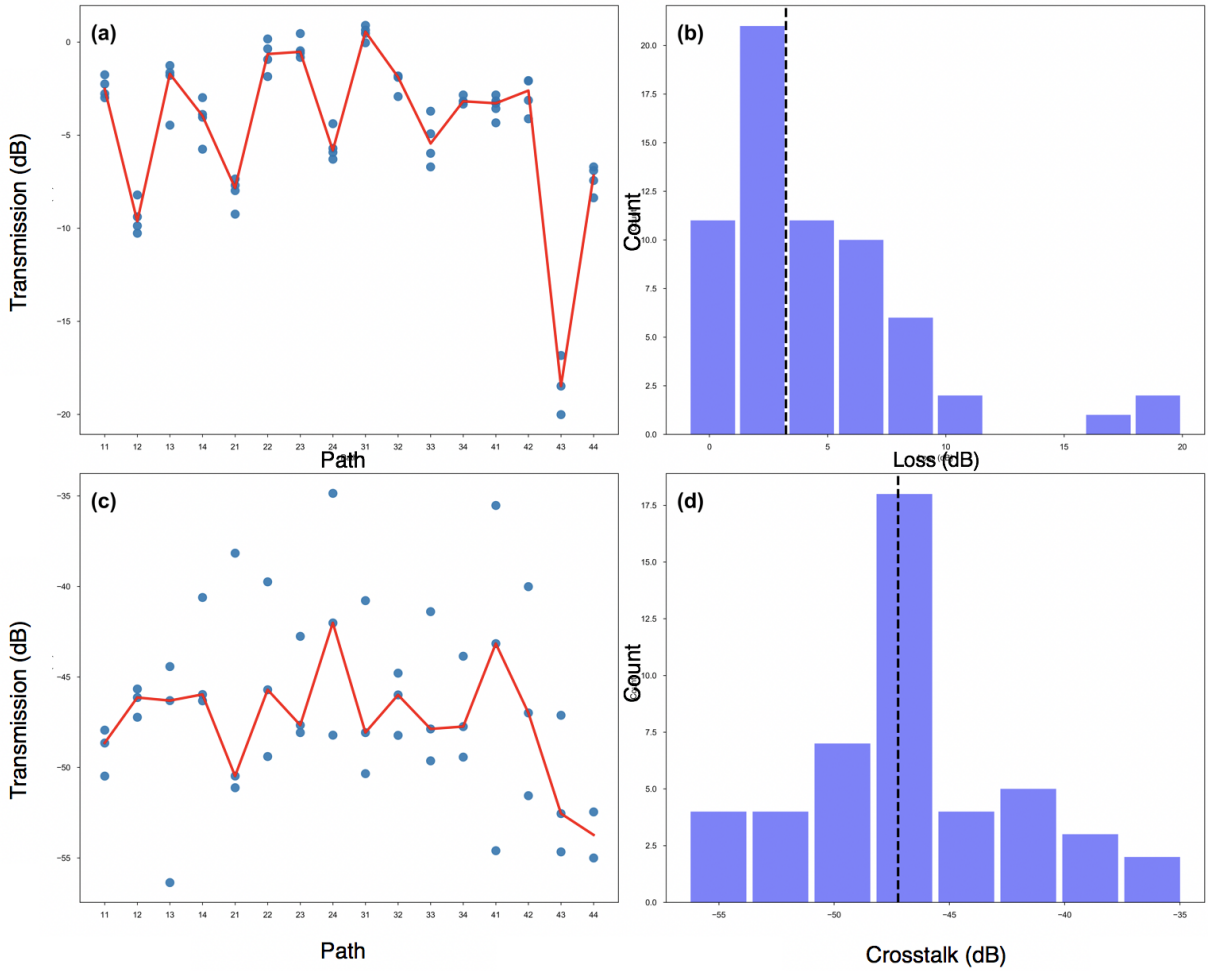

Figure 3: (a) Transmission (dB) vs. paths in the switch. Each data point (blue) corresponds to measurement at a different wavelength. Red line corresponds to line connecting medians. (b) Histogram of Loss for different paths with a median of 5.32 dB. (c) CW crosstalk is measured at 1546.8 nm. This is the signal channel. (d) Worst case crosstalk is -35 dB

 doi:10.20944/preprints202106.0426.v1

The waveguide dimension used in routing is 220 nm × 400 nm and we use 5 µm radius bends for routing all waveguides. Foundry-specified waveguide loss is 2 dB/cm and edge coupler loss is 2.7 dB/facet. A 100 µm trench is provided at the chip edge for ease of optical coupling. Waveguide crossings are designed with particle swarm optimization and have a reported average loss of 0.028 dB and worst-case crosstalk of 37 dB [16]. The designed footprint of the crossing is 17 µm x 17 µm due to 4 µm linear tapers used to taper the waveguide from 400 nm to 500 nm. Spirals with simultaneous tapered width from 400 nm to 150 nm and radius from 5 µm to 0.2 µm are used for waveguide termination. These spirals have a 20-dB reflection simulated with Lumerical 3D Finite Difference Time Domain package at 1550 nm.

Fig 3 (a) shows transmission (dB) vs. paths in the 4x4 switch. Blue dots correspond to measured data points at different wavelengths and red corresponds to median of the points for each path. Fig 3 (b) shows a median loss of 5.32 dB. Median is used instead of mean due to skewed distribution of the data. The outliers in Fig 3 (a) and (b) correspond to cascaded filters with a large difference of resonant wavelengths. Continuous wave (CW) off loss is measured at 1546.8 nm. Fig 3 (c) and (d), shows the crosstalk measurement. We set a MRR on a chosen path ring to 1546.8 nm and we measure the crosstalk power at other ports.

4 Discussion

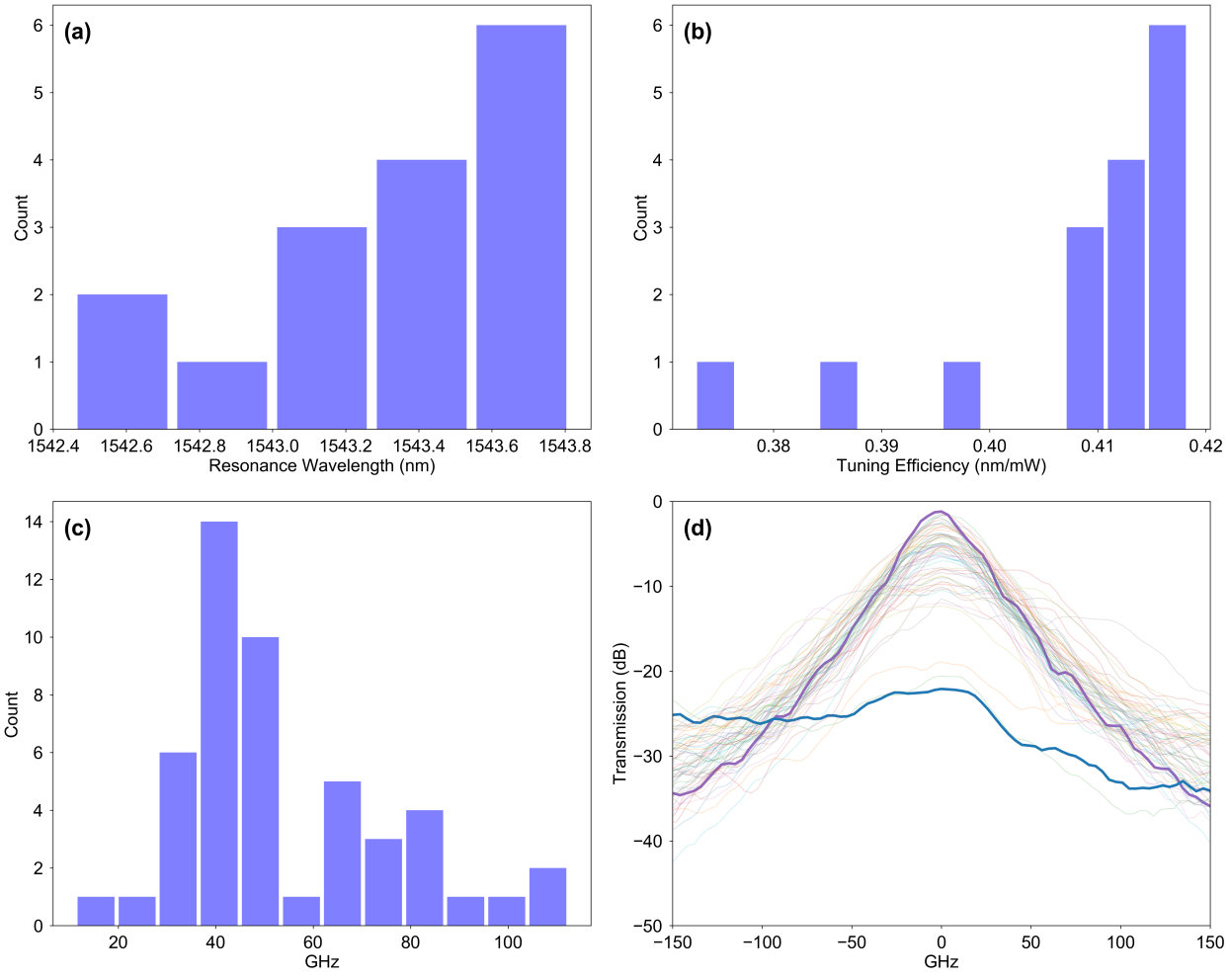

Figure 4: (a) Histogram of resonant wavelength, mean = 1543.4 and standard deviation = 0.39 nm. (b) Tuning efficiency mean = 0.41 nm/mW and standard deviation =0.012 nm/mW (c) Bandwidth histogram with median = 48.7 GHz (d) Transfer spectra of all ring resonator filters

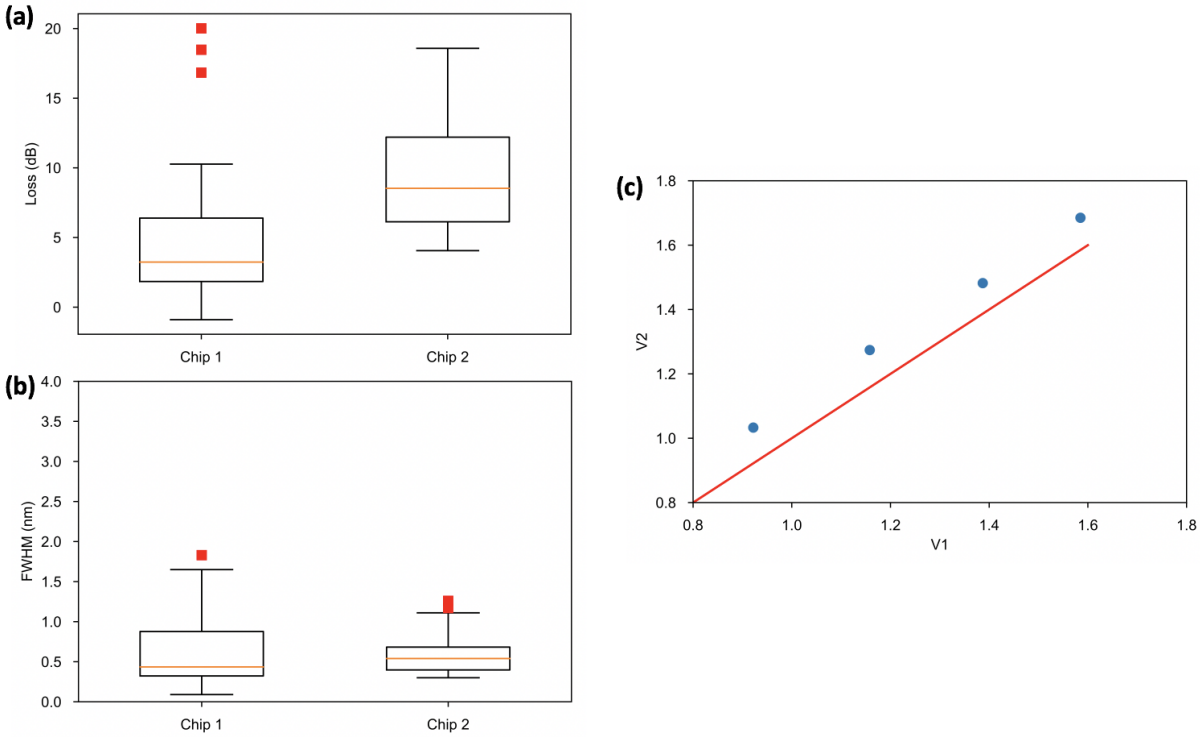

Figure 5: (a) Path loss comparison for chip 1 and chip 2. Red squares correspond to outliers and orange lines correspond to the median. (b) Full Width Half Maximum (FWHM) of different switches measured on chip 1 and chip 2. (c) A plot of voltage on each ring for maximum transmission. Red line corresponds to a 45-degree line where V1 = V2. V1 and V2 corresponds to voltages on the two MRR in a cascaded first order MRR.

Fig 4 (a) shows the histogram of resonant wavelengths with mean of 1543.4 nm and standard deviation of 0.4 nm. This is similar to the measured standard deviation of 0.3 nm for second order resonators from [4]. Fig 4 (b) shows the histogram of tuning efficiency 0.4 nm/mW and standard deviation of 0.012 nm/mW. Fig 4 (c) shows bandwidth histogram with median bandwidth of 48.7 GHz. Fig 4 (d) shows all measured transfer spectra. One can see the outlier spectra where two cascaded second order MRRs have dissimilar resonant wavelengths.

Fig. 5 (a) shows a comparison of path loss on two different chips. The orange lines correspond to the median loss. One can see that the median loss of chip 1 is 3.23 dB which is smaller than 8.53 dB of chip 2. The distribution of path losses of chip 2 is skewed towards lower values. Fig. 5 (b) shows the FWHM of chip1 and chip 2. The median FWHM of chip 1 is 0.435 nm which is smaller than 0.54 nm of chip 2. The IQR of chip 1 is 0.56 nm which is much greater than 0.29 nm of chip 2. This shows that there is a smaller variation in FWHM values. Fig. 5 (c) shows V1 and V2 applied to two rings on a test structure cascaded in the same arrangement as the rings on the switch. These voltages are optimized for maximum peak transmission of a given channel wavelength. Red line shows $V_1 = V_2$. The dissimilarity of the drive voltages could be due to two factors, variation in heater resistances or variation in the fabrication process (thickness of the chip). As the rings are placed right next to each other it is unlikely that thickness can be a factor. Different doping of resistors or other fabrication variation that can change dimensions of the resistors can change the effective index of the ring resonator. This could be the reason for different resonant wavelength and heater resistances.

5 Conclusion

We report a compact switch with same drive for two cascaded MRRs. We report a median path loss of 5.32 dB. The MRRs in the switch can tune across an entire FSR which is an improvement over our previous switches. We conclude that due to fabrication variation of current technology, we cannot drive cascaded MRRs with the same drive voltage and separate control is required.

Acknowledgement This work was supported by the U.S. Department of Defense under the AIM Photonics Manufacturing Innovation Institute, Air Force Contract FA8650-15-2-5220.

References

[1] Adel A. M. Saleh, Akhilesh S. P. Khope, John E Bowers, and Rod C Alferness. Elastic wdm switching for scalable data center and hpc interconnect networks. *OptoElectronics and Communications Conference (OECC)*, pages 1–3, 2016.

[2] Akhilesh SP Khope, Anirban Samanta, Xian Xiao, Ben Yoo, and John E Bowers. Review of integrated photonic elastic wdm switches for data centers. *arXiv preprint arXiv:2105.14934*, 2021.

[3] Xian Xiao, Roberto Proietti, Sebastian Werner, Pouya Fotouhi, and SJ Ben Yoo. Flex-lions: A scalable silicon photonic bandwidth-reconfigurable optical switch fabric. pages 1–3, 2019.

[4] Akhilesh SP Khope, Mitra Saeidi, Raymond Yu, Xinru Wu, Andrew M Netherton, Yuan Liu, Zeyu Zhang, Yujie Xia, Garey Fleeman, Alexander Spott, et al. Multi-wavelength selective crossbar switch. *Optics express*, 27(4):5203–5216, 2019.

[5] Tae Joon Seok, Jianheng Luo, Zhilei Huang, Kyungmok Kwon, Johannes Henriksson, John Jacobs, Lane Ochikubo, Richard S Muller, and Ming C Wu. Silicon photonic wavelength cross-connect with integrated mems switching. *APL Photonics*, 4(10):100803, 2019.

[6] Xian Xiao, Roberto Proietti, Gengchen Liu, Hongbo Lu, Yu Zhang, and SJ Ben Yoo. Multi-fsr silicon photonic flex-lions module for bandwidth-reconfigurable all-to-all optical interconnects. *Journal of Lightwave Technology*, 38(12):3200–3208, 2020.

[7] Akhilesh S. P. Khope, Songtao Liu, Zeyu Zhang, Andrew M. Netherton, Rebecca L. Hwang, Aaron Wissing, Jesus Perez, Franklin Tang, Clint Schow, Roger Helkey, Rod C. Alferness, Adel A. M. Saleh, and John E. Bowers. 2 λ switch. *Opt. Lett.*, 45(19):5340–5343, Oct 2020.

[8] Akhilesh SP Khope, Roger Helkey, Songtao Liu, Sairaj Khope, Rod C Alferness, Adel AM Saleh, and John E Bowers. Scalable multicast hybrid broadband-crossbar wavelength selective switch: proposal and analysis. *Optics Letters*, 46(2):448–451, 2021.

[9] Akhilesh S. P. Khope, Takako Hirokawa, Andrew M Netherton, Mitra Saeidi, Yujie Xia, Nicolas Volet, Clint Schow, Roger Helkey, Luke Theogarajan, Adel A. M. Saleh, et al. On-chip wavelength locking for photonic switches. *Optics letters*, 42(23):4934–4937, 2017.

[10] Yishen Huang, Qixiang Cheng, Anthony Rizzo, and Keren Bergman. High-performance microring-assisted space-and-wavelength selective switch. *Optical Fiber Communication Conference (OFC)*, pages 1–3, 2020.

[11] Akhilesh S. P. Khope, Roger Helkey, Songtao Liu, Adel A. M. Saleh, Rod C. Alferness, and John E. Bowers. A scalable multicast hybrid broadband crossbar wavelength selective switch for datacenters. In *2021 IEEE 11th Annual Computing and Communication Workshop and Conference (CCWC)*, pages 1585–1587, 2021.

[12] Akhilesh S.P. Khope, Songtao Liu, Andy Netherton, Zeyu Zhang, Sairaj Khope, Roger Helkey, Adel A.M. Saleh, Rod C. Alferness, and John E. Bowers. Experiments on multiwavelength selective crossbar switches. In *2020 International Conference on Information Science and Communications Technologies (ICISCT)*, pages 1–5, 2020.

[13] Akhilesh S. P. Khope, Adel A. M. Saleh, John E Bowers, and Rod C Alferness. Elastic wdm crossbar switch for data centers. *IEEE Optical Interconnects (OI) Conference*, pages 48–49, 2016.

[14] Akhilesh SP Khope. Lumos: A python instrument control library for photonics. 2021.

[15] Akhilesh SP Khope. Ultralow loss adiabatic microring resonator with thermal tuning. 2021.

[16] Yangjin Ma, Yi Zhang, Shuyu Yang, Ari Novack, Ran Ding, Andy Eu-Jin Lim, Guo-Qiang Lo, Tom Baehr-Jones, and Michael Hochberg. Ultralow loss single layer submicron silicon waveguide crossing for soi optical interconnect. *Optics express*, 21(24):29374–29382, 2013.